FLIGHT PATH ANALYSIS IN SOUNDING ROCKET "LIBERTADOR I" WITH COMPUTATIONAL SIMULATION ON THREE DEGREES OF FREEDOM

J. Murcia[a] S. Gómez[b] H. Cerón-Muñoz[c] y G. Portilla[d]

[a] Ingeniería y Tecnologías Espaciales - Instituto Nacional de Pesquisas Espaciais INPE.
Av. dos astronautas 1758, Jd. Granja – CEP 12227-010.
São José dos Campos – SP. Brasil.
Email: jhonathan.pineros@inpe.br, jomurciap@unal.edu.co
[b]Departamento de Ingeniería Aeronáutica – Fundación Universitaria Los Libertadores.
Bogotá – Colombia.
Email: sagomezs@libertadores.edu.co
[c]Escuela de Ingeniería de São Carlos – Universidad de São Paulo - EESC - USP
Departamento de Ingeniería Aeronáutica. São Carlos – Brasil.
Email: hernan@sc.usp.br
[d]Observatorio Astronómico Nacional – Universidad Nacional de Colombia – OAN - UNAL.
Bogotá – Colombia.
Email: jgportillab@unal.edu.co

ABSTRACT

This paper presents obtained results from computer simulations in order to analyze the flight path of the sounding rocket Libertador I, developed in 2012 at the Fundación Universitaria Los Libertadores. The main aspects that affect the motion of a rocket are propulsion and aerodynamics effects. Numerical algorithms were implemented to value the thrust provided by the rocket motor as well as aerodynamic loads. Then, the differential equations of the motion are solved using the Runge-Kutta method, RK9. Trajectory and other numerical results are calculated from a code developed in FORTRAN. Finally, graphs of the flight path, curves of the vehicle velocity as function of time are presented. Also, the algorithm permits to determine the maximum altitude and possible impact sites.

Key Words: Flight path, flight simulation, rocket motor, solid propellant, sounding rocket.

1. INTRODUCTION

Sounding rocket is an experimental aerospace vehicle used in helio-physics, astronomy and earth sciences. It has a suborbital flight path reaching supersonic speeds and is powered by one or more rocket motors [8]. Since 2012, *Fundación Universitaria Los Libertadores* has been developing a research project about the design and construction of a sounding rocket, named *Libertador I*. The mission of this rocket is to transport an atmospheric data computer from the earth surface to the troposphere or stratosphere [6]. The project has the support of the *Escola de Engenharia de Sao Carlos – EESC, Universidad de Sao Paulo – USP* in Brazil.

1.1. Rocket motor

Libertador I will be propelled by a solid rocket motor; the motor can generate up to 184 kg of thrust with a propellant mass of 5 kg, its dimensions are 64 mm on outside diameter and 0,9 m of length. The combustion chamber is made of aluminum alloy, 2024-T3. The solid propellant generates the necessary energy for the lift-off, it contain potassium nitrate - KNO_3 in 65%, molar fraction, and Dextrose - DX in 35%. The amount of gas ejected varies in time due to the geometry and the projected area of the propellant bar. The fundamental equation that describes the behavior of the total thrust on the rocket motor systems Eq. 1 is defined as [11]:

$$T = \dot{m}V_e + A_e(P_e - P_a),$$ (1)

Where, T is the total thrust, which depends of the product between the mass flow $\dot{m}$, gas ejected, and the exhaust velocity V_e on the nozzle exit A_e, this term is named momentum thrust. The right side of equation shows an additional term called aerodynamic thrust, it is defined by the exit area A_e, static pressure P_e , on the nozzle exit and the atmospheric pressure P_a, the last one change with the altitude.

1.2. Rocket aerodynamics and recovery system

Another aerodynamic device for the rocket mission is the parachute or recovery system, it is ejected at the highest point of flight trajectory, apogee. The objective of the parachute is to increase the drag force in order to reduce the impact velocity, thus, recovery and reuse is possible. With a CAD model of system rocket-parachute, an analysis CFD is conducted to valuate aerodynamic loads under different velocities. The rocket geometry should minimize drag forces, for this reason it has three delta wings with supersonic diamond airfoils, a boat tail, and a Von-Karman ogive of 381 mm in length and a diameter 38,1 mm. The complete geometry of the rocket is showed in the figure 1 [6].
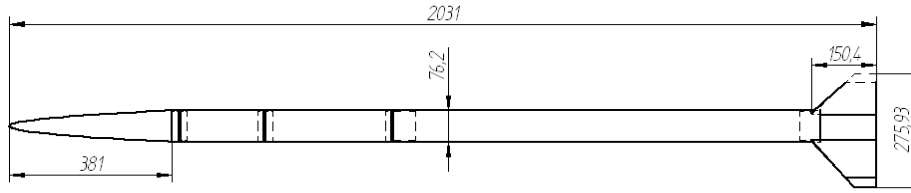

Figure 1. Rocket geometry in millimeters.

1.3. Rocket flight dynamics

The equation that governs the rocket motion includes every force acting on the body. The local reference system is formed by the normal and tangential components of the velocity vector. The system is shown in figure 2.
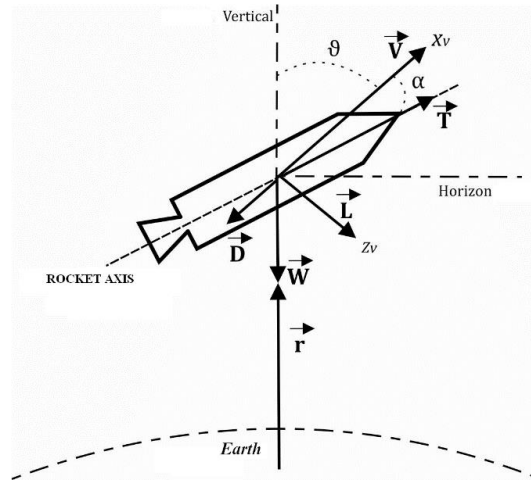

Figure 2. Forces diagram on the rocket body.

The six first-order differential equations Eq. 2 at Eq. 7, which govern rocket motion in three degrees of freedom, 3 DOF, from inertial system (fixed at Earth center), can be written as [12, 13]:

$$\dot{\phi} = \frac{v \sin \vartheta \cos A}{r}, \tag{2}$$

$$\dot{\lambda} = \frac{v \sin \vartheta \sin A}{r \cos \phi}, \tag{3}$$

$$\dot{r} = v \cos \vartheta , \tag{4}$$

$$\dot{v} = \frac{T \cos \alpha}{m} - \frac{D}{m} - \frac{W \cos \vartheta}{m} - \omega^2 r \cos \phi (\cos A \sin \phi \sin \vartheta - \cos \phi \cos \vartheta), \tag{5}$$

$$\dot{\vartheta} = \frac{T \sin \alpha}{mv} + \frac{L}{mv} + \frac{W \sin \vartheta}{mv} - \dot{\psi} - \frac{\omega^2 r \cos \phi}{v} (\sin \phi \cos \vartheta \cos A + \cos \phi \sin \vartheta), \tag{6}$$

2

$$\dot{A} = \frac{v \sin\vartheta \tan\phi \sin A}{r} + \frac{\omega^2 r \sin\phi \cos\phi \sin A}{v \sin\vartheta} - \frac{2\omega(\cos\vartheta \cos\phi \cos A - \sin\vartheta \sin\phi)}{\sin\vartheta} \, , \quad (7)$$

Where r is the radial vector, v is velocity, α is angle of attack, ϕ and λ are latitude and longitude angles, ϑ is flight path angle, A is azimuth angle from the Earth's geometric north to the east, W is the rocket weight that change on the time, D is aerodynamic drag force, L is lift force and T is the thrust force. The last three equations include the angular velocity of the Earth in the equator, ω, which generate Coriolis and centripetal forces [9, 10, 14]. Equations 2 to 7 are mutually coupled and is necessary a computational code to solve them.

As the vehicle moves through the Earth's atmosphere, aerodynamic forces of drag and lift change due to the variation of air density with altitude. Therefore, is necessary to implement a standard atmosphere model such as US1976 [1, 5].

2. METHODOLOGY

This section presents the computational methods for solving differential equations mentioned above.

2.1. Numerical integrator

The numerical integration of Runge-Kutta - RK9 was implemented in order to resolve the differential equations of three degrees of freedom. The method used is an implicit runge-kutta method (RADAU) of order 15 known as RA15 which is used in the solution of differential equations in celestial mechanics [9]. The computer code is written in FORTRAN, it includes data from the thrust provided by the rocket motor and the aerodynamic coefficients. The time step that is used in the integrator is 1ms. The implemented algorithm is a variant of another one that analyzes the flight path of space launch vehicles developed in the ObservatorioAstronomico Nacional - OAN from University Nacional de Colombia - UNAL [7].

3. Results and discussion

3.1. Thrust force as function of time

Inner geometry of the rocket and the solid propellant determinates the thrust force in function of time on conditions of sea level, Fig. 3. These results are included in the code for modeling mass and the thrust force for each instant of time. With the mass flow, the net weight of the rocket can be calculated.
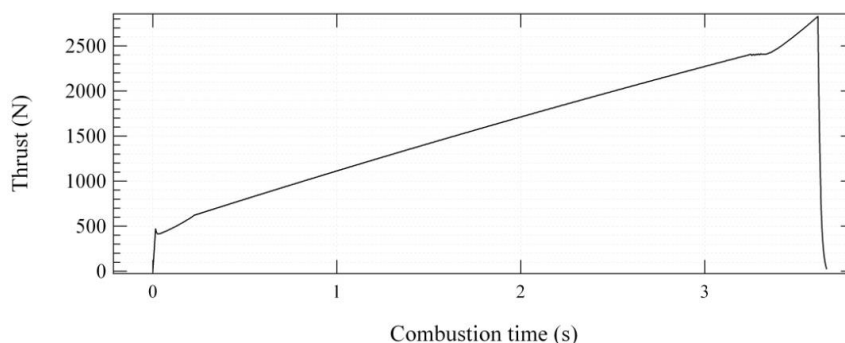

Figure 3. Thrust vs. combustion time solid propellant rocket motor.

3.2. Drag coefficients

Supersonic speeds are generated on the flight path of the rocket. In the Fig. 4 is plotted the drag coefficient of the body as a function of Mach number, considering that in this case the value of the angle of attack is constant and equal to 0º; it does not take into account the rotation of the rocket or the influence of crosswinds [7]. Like the thrust force, the results of the aerodynamics loads obtained by CFD are added to the flight path code as a subroutine.
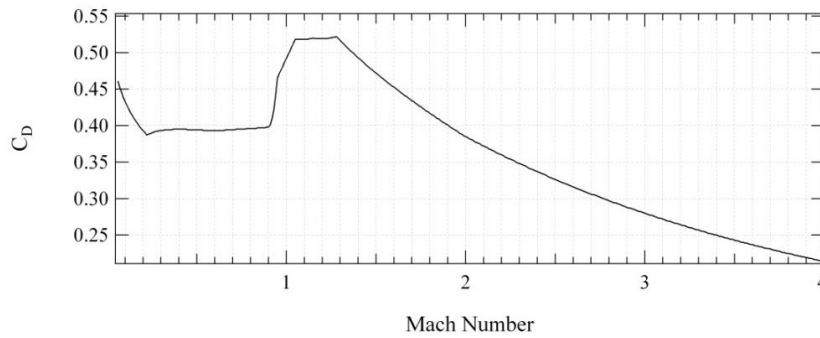
Figure 4. Rocket drag coefficient with AOA 0º vs. Mach number.

3.3. Flight path

Rocket flight was simulated in the computer code under two cases: launched vertically and with the opening of its parachute at the apogee. The moments of inertia in the rocket body are not taken into account, because it is not a simulation of 6DOF; it does not have any control over the rocket body, phenomenon caused by winds are neglected, an ideal atmosphere is assumed, and its angle of attack during the entire flight path is equal to 0°. Also, pitching moments caused by the change of the center of gravity - GC due to the consumption of propellant are neglected.

The first variable taken into account is the change of the mass versus time. As was mentioned, the mass flow is variable because the burning area of the propellant is not constant. The initial mass of the rocket is 10 kg and when the propellant is consumed it descends to 5 kg, Fig. 5.
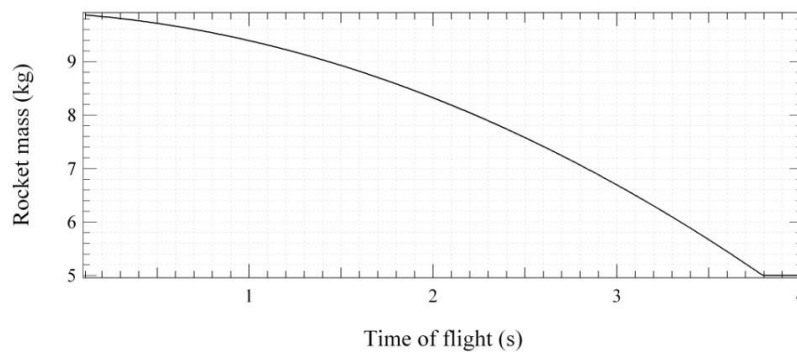

Figure 5. Rocket mass vs time.

3.3.1. Variation on Flight Path Angle (FPA).

Gaori, located in Colombia, was chosen as a possible launch site for the sounding rocket. Its coordenades are: longitude of 68°41'08¨ W and latitude of 05°31'28¨ N. Military and academic rockets have been previously tested in this place [3]. First, the flight path is analyzed under the influence of changes in FPA at launch with a constant azimuth of 90° (west-east), initial mass 10 kg, final mass 5 kg, without payload, and ballistic flight without parachute or recovery system. The changes in FPA goes from 0º to 45º with intervals of 15º. Figure 6 shows that the maximum altitude or apogee is under 22 km with 0º FPA and flight time around 140 s. Similarly, it is observed that increasing the FPA decreases flight time and altitude (apogee).

Behavior of the total velocity of rocket is obtained too, as is shown in Fig. 7, where the minimum velocity is achieved in the apogee with 0º FPA. This path is ideal to operate the parachutes. Also, the plots of the figure 7 show that the velocity increases as the system loses mass and reaches its peak at the end of combustion, after it begins to go down until to reach the apogee, where gravitational attraction causes the body starts to fall, increasing its velocity to the point where the air density is greatest and aerodynamic drag increases due to dynamic pressure (Fig. 8), without parachutes, the rocket descent at supersonic speeds. Similar to Fig. 7, Fig. 9 shows the Mach number as a function of

4

time, considering that the speed of sound changes with the altitude and temperature of the atmosphere. The maximum Mach reached by the rocket is 3.5 approx.
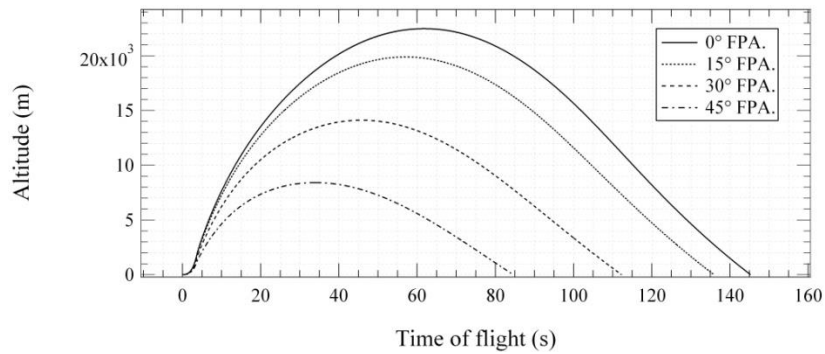

Figure 6. Altitude vs. time flight as function of FPA.
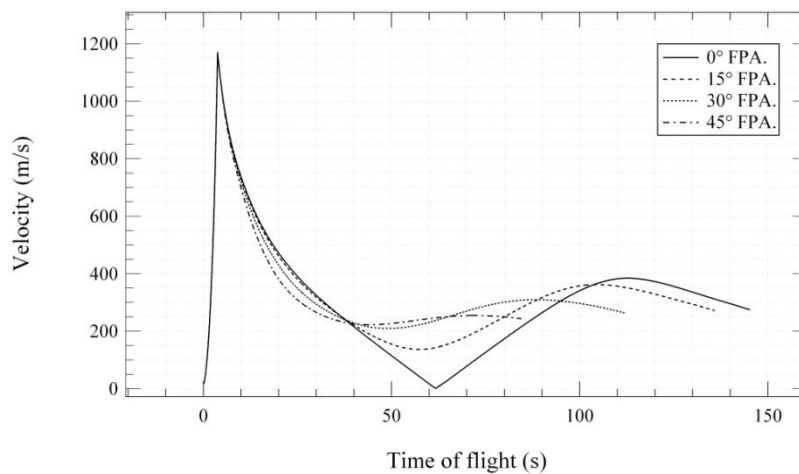

Figure 7. Velocity vs. time flight as function of FPA.

Figure 8 shows that the maximum dynamic pressure is achieved at the end of combustion too, where it reaches a value greater than seven times the atmospheric pressure at sea level, it is the design load to be supported by the structure, then the dynamic pressure decays as the rocket descends into the Earth's atmosphere.
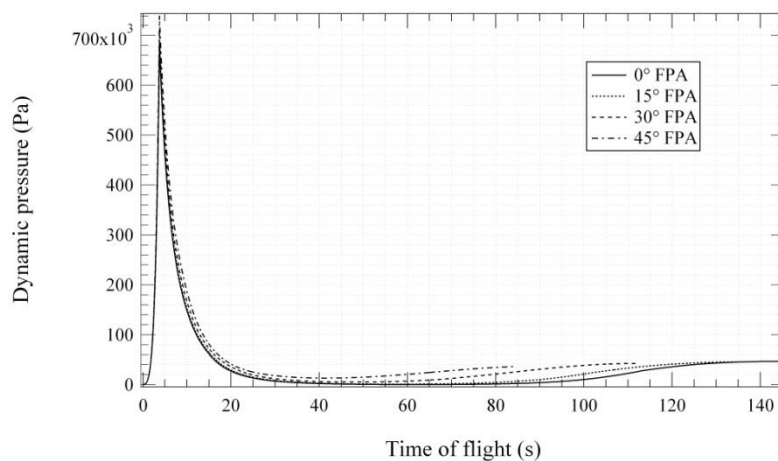

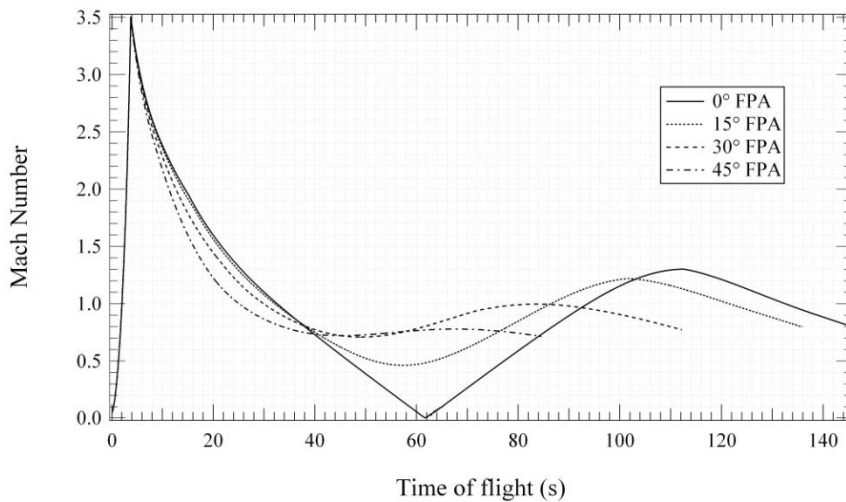**Figure 8**. Dynamic pressure vs. time of flight as function of FPA.

Figure 9. Mach number vs. time of flight as function of FPA.

Acceleration is valuated with the ratio absolute acceleration of the vehicle to gravity, a/g, see Fig. 10. This number increases as the rocket loses mass and increases its thrust force and is proportional to the ratio thrust-weight (T/W). Both, structure and payload are submitted until 35 g approx. Then, without propulsion the acceleration of the vehicle reaches the nominal gravity.
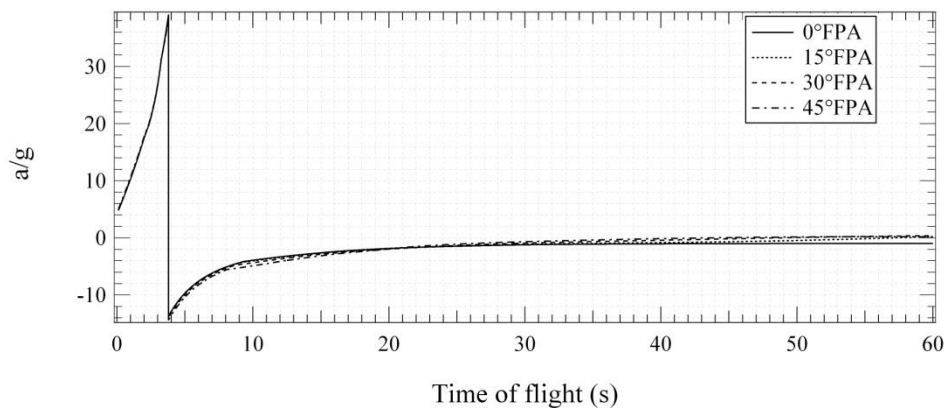

Figure 10. a/g ratio vs. time of flight.

Ballistic tables are made to predict the maximum horizontal range in function of the FPA at launch, allowing locates the impact zone and determine the maximum altitude. The figure 11 shows that the maximum range is obtained with 30° FPA. It is a effect of the variable density in the atmosphere, usually, this angle is 45°.
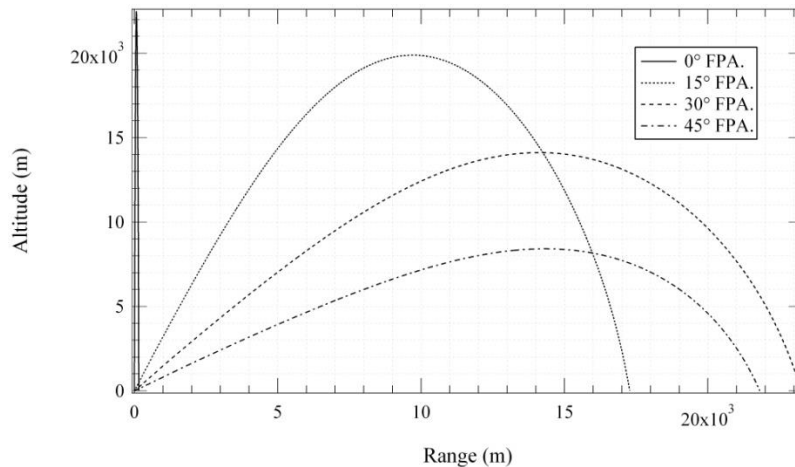

Figure 11. Altitude vs. range with variations in FPA.

3.3.2. Payload mass.

After conducting computer simulations with variation in the angles of flight path trajectory, the flight of the rocket was simulated with a FPA of 0° at lift-off, 90° constant azimuth and varying the mass of the payload from 0 kg to 2 kg to determine the influence of the mass in the flight path. Figure 12 shows the vehicle reaches the highest altitude with a 0 kg payload and 10 kg total mass at liftoff. The difference between the apogees of the path with the highest payload and without payload is 4 km approx.
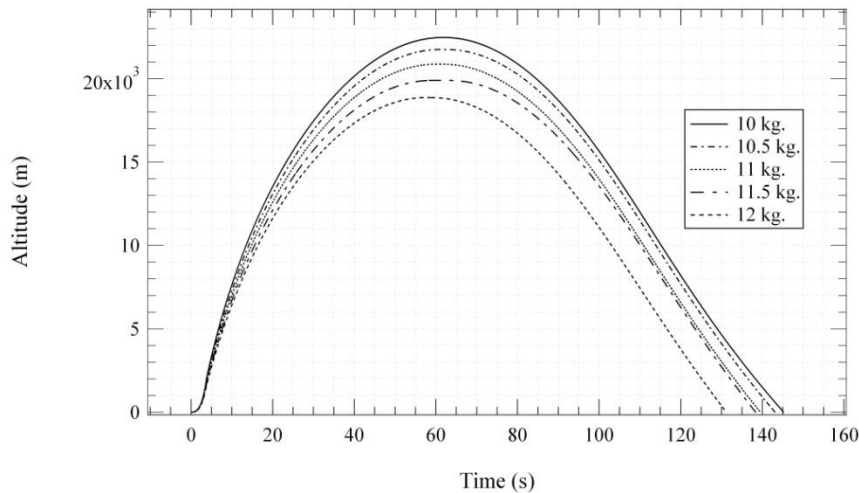

Figure 12. Altitude vs time of flight with variation in payload mass.

In the velocity plot, is observed that in the unloaded vehicle develops almost 50 m/s more than when the vehicle transports 2 kg of payload, as the payload is increased, velocity and vertical range decreases, see Fig. 13.
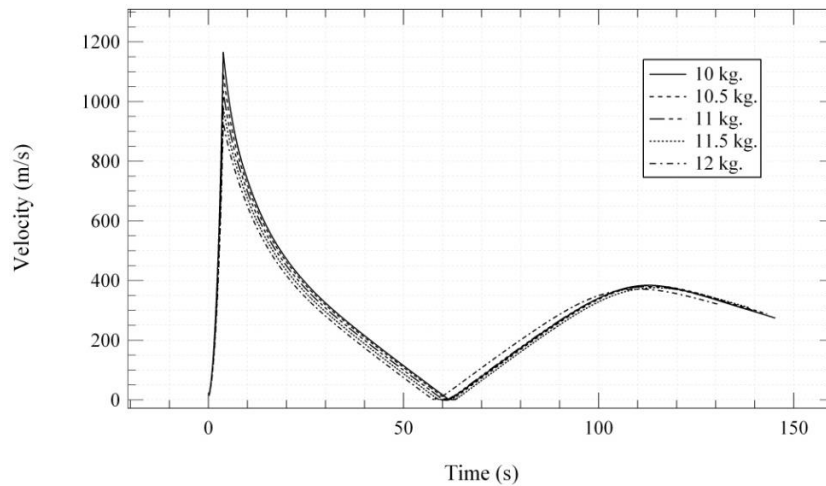

Figure 13. Velocity vs. time with variation in payload mass.

3.3.3. Flight path with recovery system.

The sounding rocket has a parachute recovery system with aerodynamic braking. The simulations were developed with this system. In this case the rocket incorporates a hemispherical parachute with area of 2,5 m^2 and CD≈0,6 which is deployed at the apogee [2] This element allows for recovering the vehicle with its payload at a controlled rate of descent around to 8 m/s, to avoid structural damage on the impact instant (see Fig. 14), this systems increasing the flight time close to 1.600 s.
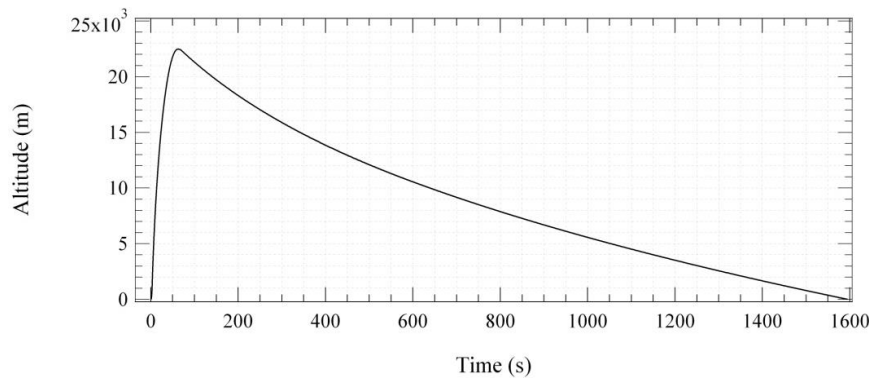
Figure 14. Altitude vs. time of flight with recovery system.

3.3.4. Impact zones

Given the coordinates of the possible launch site were simulated a series of flight paths with 45° FPA without payload or parachute, were varying the azimuth angle from 0° to 360° at 15° to get the coordinates of the impact point located nearly 22 km from the launch site. In Figure 15are observed coordinates of impact zones.
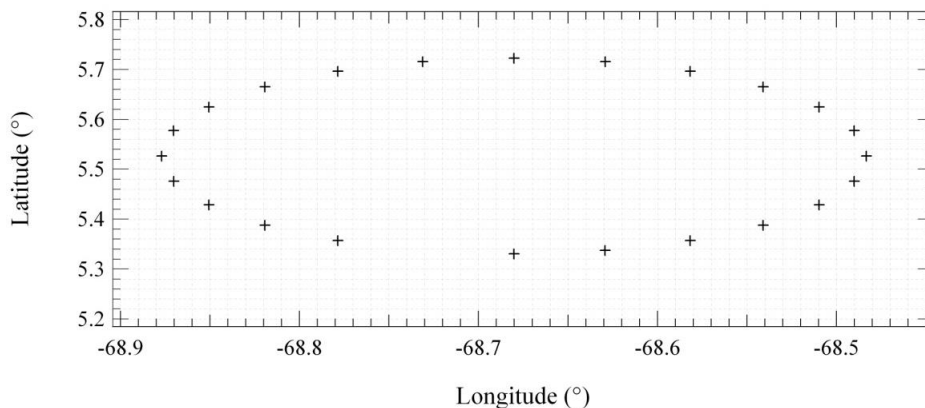

Figure 15. Impact zone coordinates.

4. Conclusions

The use of computational codes to predict the partial performance of the rocket during its flight helps to validate the design of the vehicle and learn the operating ranges to which instruments onboard will be subjected, payload and systems recovery. It is expected to corroborate the results of the simulations with experimental data obtained in the systems, including the rocket engine implementation in a test stand that is being developed by the group, the wind tunnel data in scale models of rocket for the aerodynamic and real trajectory data from flight computers and payload.

The design of this sounding rocket serves to perform many experiments in diverse areas of study such as supersonic aerodynamics, dynamic aerospace structures, propulsion, aerospace medicine, among others.

The results of the simulations are used to determine the best operating conditions of the vehicle at the time of its release, according to the payload to be transported and the experiment to be performed, for example, in the first flight will be transport a mass of 0,5 kg from the data computer to collect temperature, humidity and atmospheric pressure data, in this case is select a launch with 0° FPA and can estimate the maximum altitude obtained through simulations with 10,5 kg of total liftoff mass.

The development of these projects is very beneficial to the integration of professionals in various areas of knowledge, being a productive exercise for an educational institution. There are not antecedents about this kind of project in Colombia, so the computer simulations shows, first, an approximation regarding the performance of the rocket, which allows validation and improvement in some systems both subsystems in the design stage without having to spend resources on production and testing.

Additionally, a computational code with 6DOF and 9DOF simulations should be include once the vehicle would be built and assembled, after which we proceed to verify the results of the simulations with the flight of the rocket that is expected to be in 2015.

Acknowledgements

REFERENCES

1. Anderson, J., 2010, "Introduction to Flight". McGraw Hill 6ª. ed. New York.

2. Cerón-Muñoz, H. D.,*et. al.*,2012, "Modelación Dinámica del Sistema de Recuperación de un Cohete". Universidad Distrital Francisco José de Caldas. *Cuarto Congreso Internacional en Ciencia y Tecnología Aeroespacial CICTA 2012*. Bogotá.

3. Gutiérrez, R., 2012, "Programa Espacial de la Fuerza Aérea Colombiana (FAC), Avances y Proyección". Universidad Distrital Francisco José de Caldas. *Cuarto Congreso Internacional en Ciencia y Tecnología Aeroespacial CICTA 2012*. Bogotá.

4. Humble, R., Henry, G., and Larson, W., 1995. "Space Propulsion Analysis and Design". McGraw Hill 3ª. ed. New York.

5. Minzner, R., Champion, K., and Pond, H., 1959, "The ARDC model atmosphere, 1959". Air Force Surveys in Geophysics No 115. Cambridge. England.

6. Murcia, J.O.,*et. al*., 2012. "Diseño Conceptual, Preliminar y Análisis de la Trayectoria de Vuelo de un Cohete Sonda de Propelente Solidó para Carga Útil de 2 kg". Universidad Distrital Francisco José de Caldas. *Cuarto Congreso Internacional en Ciencia y Tecnología Aeroespacial CICTA 2012*. Bogotá.

7. Murcia, J.O., 2012, "Estudio de la Trayectoria de un Cohete de Tres Etapas Lanzado desde el Territorio Colombiano". Tesis de Maestría en Ciencias Astronomía. Universidad Nacional de Colombia. Bogotá.

8. NASA, 2011. National Aeronautics and Space Administration. "Sounding Rockets 2011 Annual Report". Goddard Space Flight Center. 1ª. ed. Wallops Island. Virginia.

9. Portilla, J.G., 1996, "El Problema de los dos Cuerpos y el Problema Principal del Satélite Artificial en Ecuaciones Diferenciales de Primer Orden". *Revista Academia Colombiana de Ciencias*. Vol. 20. No. 76. pp. 25-32.

10. Portilla, J.G., 2009. "Elementos de Astronomía de Posición". Unibiblos. 1ª.ed. Bogotá.

11. Sutton, G.P. and Biblarz, O., 2010. "Rocket Propulsion Elements". Jhon Wiley and Sons, Inc. 8ª. ed. New York.

12. Tewari, A., 2006. "Atmospheric and Space Flight Dynamics". Birkhauser. 1ª. ed. Berlin.

13. Weiland, C., 2010. "Computational Space Flight Mechanics". Springer. 1ª. ed. Berlin.

14. Zipfel, P., 2007,"Modeling and Simulation of Aerospace Vehicle Dynamics". AIAA. 2ª. ed.